

**LIG climate and
Greenland Ice Sheet
melting**

P. Bakker et al.

Sensitivity of the North Atlantic climate to Greenland Ice Sheet melting during the Last Interglacial

P. Bakker, C. J. Van Meerbeek, and H. Renssen

Section Climate Change and Landscape Dynamics, Department of Earth Sciences, VU University Amsterdam, De Boelelaan 1085, 1081 HV Amsterdam, The Netherlands

Received: 9 August 2011 – Accepted: 23 August 2011 – Published: 31 August 2011

Correspondence to: P. Bakker (p.bakker@vu.nl)

Published by Copernicus Publications on behalf of the European Geosciences Union.

This discussion paper is/has been under review for the journal Climate of the Past (CP).
Please refer to the corresponding final paper in CP if available.

Title Page

Abstract

Introduction

Conclusions

References

Tables

Figures



Back

Close

Full Screen / Esc

Printer-friendly Version

Interactive Discussion



Abstract

During the Last Interglacial (LIG; ~130 thousand years BP), part of the Greenland Ice Sheet (GIS) melted under the influence of a warmer than present-day climate. However, the impact of this melting on the LIG climate in the North Atlantic region is unknown. Using the LOVECLIM earth system model of intermediate complexity we have systematically tested the sensitivity of the LIG climate to increased freshwater runoff from the GIS. Moreover, additional experiments have been performed to investigate the impact of an idealized reduction of both altitude and extent of the GIS on the LIG climate. By comparing the simulated deep ocean circulation with proxy-based reconstructions, the most realistic simulated climate could be discerned. The resulting climate is characterized by a shutdown of deep convection in the Labrador Sea and a subsequent cooling here by ~6 °C and ~2 °C over the southern part of Baffin Island and the North Atlantic Ocean between 40° N and 60° N. The reduction of altitude and extent of the GIS results in a local warming of up to 6 °C and a reduction in deep convection and accompanying cooling in the Nordic Seas. Combining model results and proxy-based reconstructions enabled us to constrain the possible melt rate of the GIS to a flux between 0.052 Sv and 0.13 Sv. A further comparison of simulated summer temperatures with both continental and oceanic proxy-records reveals that the partial melting of the GIS during the LIG could have delayed maximum summer temperatures in the western part of the North Atlantic region relative to the insolation maximum.

1 Introduction

Measurements and modelling studies predict that the Greenland Ice Sheet (GIS) is likely to partially melt in the future (Rignot et al., 2011; Driesschaert et al., 2007) under the influence of a warmer climate (Solomon et al., 2007). The implications of enhanced GIS melting are a central theme in the current climate change debate, not only because of potential sea-level rise, but also because of the possible impact on

CPD

7, 2763–2801, 2011

LIG climate and Greenland Ice Sheet melting

P. Bakker et al.

Title Page

Abstract

Introduction

Conclusions

References

Tables

Figures

⏪

⏩

◀

▶

Back

Close

Full Screen / Esc

Printer-friendly Version

Interactive Discussion



LIG climate and Greenland Ice Sheet melting

P. Bakker et al.

Title Page

Abstract

Introduction

Conclusions

References

Tables

Figures

⏪

⏩

◀

▶

Back

Close

Full Screen / Esc

Printer-friendly Version

Interactive Discussion



the ocean circulation. However, the relationship between enhanced GIS melting and the ocean circulation is not well understood (Swingedouw and Braconnot, 2007). It is therefore crucial to study the impact of GIS melting on the warmer than present-day Last Interglacial (LIG, 130 to 116 ka BP) climate (CAPE-members, 2006) during which the GIS was as well significantly reduced in size (Alley et al., 2010).

Since a negative GIS mass balance is accompanied by a relatively larger freshwater flow into the surrounding oceans, this would lower the density of the surface ocean waters and could therefore influence the Atlantic Meridional Overturning Circulation (AMOC). As the AMOC transports warm and saline waters from the equator northwards along its wind and density-driven upper limb (Broecker et al., 1990; Schmitz, 1995), changes in its heat transport may greatly impact temperatures in regions like northwestern Europe (Kuhlbrodt et al., 2007). In the subpolar North Atlantic Ocean these surface waters are sufficiently cooled until they overcome the vertical density gradient in the water column. At that point deep convection occurs forming North Atlantic Deep Water (NADW), a high density water mass flowing southward at depth (Schmitz, 1995; Weaver et al., 1999). Nowadays, NADW is formed in two regions, the Labrador Sea and the Nordic Seas, where respectively Labrador Sea Water (LSW) and Nordic Seas Deep Water (NSDW) are formed. Deep convection leading to NADW production further occurs in the Irminger Sea but its importance for the AMOC is not yet fully established (Bacon et al., 2003).

Experiments with different climate models of low to intermediate complexity indicate that the AMOC is a highly non-linear system with multiple equilibrium states, and typical hysteresis behaviour in response to changes in the freshwater budget of the Atlantic region (Rahmstorf, 1995; Rahmstorf et al., 2005). Although hysteresis is a common feature in these types of models, their sensitivity to a change in the freshwater budget differs greatly, as does the proximity of the present-day climate to the bifurcation point (Stommel, 1961; Rahmstorf et al., 2005). In some models it takes less than 0.1 Sv of freshwater to substantially weaken the AMOC, while in others more than 0.5 Sv is needed (Rahmstorf et al., 2005). The non-linear relationship between changes in the

freshwater budget of the North Atlantic and the overturning circulation has also been suggested by geological data. An example is the Holocene 8.2 ka BP cooling event, in which the AMOC was weakened by a catastrophic release of meltwater from glacial lakes Agassiz and Ojibway (Barber et al., 1999; Renssen et al., 2001). However, while modelling studies have shown that the relationship between changes in the freshwater budget and the AMOC strongly depends on the exact region which is perturbed (Smith and Gregory, 2009; Roche et al., 2010), the impact of changes in the mass balance of the GIS, possibly a critical region in the near future, is still largely unknown.

The future evolution of the GIS under the influence of different greenhouse gas scenarios and the resulting impact on the freshwater runoff and ocean circulation has been simulated by Driesschaert et al. (2007) and Ridley et al. (2005) using coupled climate-ice-sheet models. Both show that the GIS is likely to lose mass but a noticeable weakening of the AMOC is only found for a very strong increase of greenhouse-gas concentrations (i.e. the upper range of IPCC climate change scenarios; Solomon et al., 2007). Modelling the evolution of the GIS during the LIG using a similar approach, Otto-Bliesner et al. (2006) also found a slightly reduced AMOC when the North Atlantic is forced by enhanced melting of the GIS. A shutdown of the overturning circulation under the influence of GIS melting has thus far not been found in modelling studies, indicating that this is not a likely scenario, neither for the near future nor the LIG. However, it has been suggested that in climate models the sensitivity of the AMOC to changes in the freshwater budget is systematically too low (Hofmann and Rahmstorf, 2009).

Because the relationship between GIS melting and the AMOC is highly model dependent, it is important to constrain modelling results with proxy-based reconstructions. For example, reconstructions of the deep ocean circulation and reconstructions of the magnitude and duration of enhanced GIS melting can be used to constrain modelling results for the LIG period. Reconstructions of ocean circulation show that deep convection in the Nordic Seas was probably comparable to the present-day interglacial situation, but the timing of maximum strength is under debate (Cortijo et al., 1994,

LIG climate and Greenland Ice Sheet melting

P. Bakker et al.

Title Page

Abstract

Introduction

Conclusions

References

Tables

Figures



Back

Close

Full Screen / Esc

Printer-friendly Version

Interactive Discussion



2006), these back of the envelope calculations of possible melt rates stress the urgency to cover a large range of scenarios.

Because of the difficulties listed above – model dependent climate sensitivity, uncertainty in reconstructions of both past ocean circulation and the evolution of the GIS meltwater flux – the impact of GIS melting on AMOC and climate must be assessed systematically. Therefore, we performed a suite of 24 climate simulations in which an early LIG climate state is perturbed by different GIS melt rates – ranging from 0.0065 Sv to up to 0.299 Sv ($1 \text{ Sv} = 10^6 \text{ m}^3 \text{ s}^{-1}$) – with the LOVECLIM three-dimensional earth system model. To further investigate the climatic impact of a lower elevation and decreased extent of the GIS as a consequence of its partial melting, we carried out additional sensitivity experiments. We will focus on both the impact of GIS melting on the deep ocean circulation and on the impact on the surface climate in the North Atlantic region. Model results are then summarized by defining key regions in which the simulated July surface air temperature anomaly is sufficiently large to potentially be detected in geological records. In a second step, a range of most plausible melt rates of the GIS during the LIG is selected by comparing the simulated deep ocean circulation with proxy-based reconstructions. Finally, with this constraint on the GIS melt rate, we attempt a first comparison of the surface temperatures in simulations and proxy-data to quantify the climate impact of GIS decay during the early-LIG.

2 Model and experimental setup

We have used the Earth system model of intermediate complexity (EMIC) LOVECLIM (version 1.2; Goosse et al., 2010) which includes a representation of the atmosphere, the ocean and sea-ice, the land-surface and its vegetation. The atmospheric component is ECBilt (Opsteegh et al., 1998), a spectral T21, three-level quasi-geostrophic model. The sea-ice-ocean component is CLIO3 (Goosse and Fichefet, 1999), consisting of a free-surface primitive equation model with a horizontal resolution of 3° longitude by 3° latitude and 20 vertical levels. The vegetation module is VECODE (Brovkin et al.,

CPD

7, 2763–2801, 2011

LIG climate and Greenland Ice Sheet melting

P. Bakker et al.

Title Page

Abstract

Introduction

Conclusions

References

Tables

Figures

◀

▶

◀

▶

Back

Close

Full Screen / Esc

Printer-friendly Version

Interactive Discussion



2002) in which dynamical vegetation changes are simulated in response to climatic conditions. In this study no interactive ice-sheet model was used. We could therefore fully control the altitude, extent and the meltwater coming from the GIS and thus separately study the climatic impact of the different processes accompanying a melting GIS.

The climate sensitivity of LOVECLIM1.2 to a doubling of the atmospheric CO₂ concentration is at the lower end of the range found in global climate models (1.9°C after 1000 yr; Goosse et al., 2010). The simulated deep ocean circulation in LOVECLIM1.2 compares reasonably well with other model results with a maximum overturning streamfunction in the North Atlantic of 22 Sv and an export towards the Southern Ocean of 13 Sv and as observed over the last decades, deep convection takes place in both the Nordic Seas and the Labrador Sea (Goosse et al., 2010). The present-day deep ocean circulation in LOVECLIM1.2 is somewhat more sensitive to perturbations of the freshwater budget (Goosse et al., 2010) than an earlier version of the model (namely ECBilt-CIIO), a version for which the sensitivity was found to be very similar to coupled atmosphere-ocean general circulation models (AOGCMs; Rahmstorf et al., 2005). Model-data comparison for different climatic settings like the 8.2 ka BP event (Wiersma and Renssen, 2006) and the last deglaciation (Renssen et al., 2009), showed that the sensitivity of the AMOC to a perturbation of the freshwater budget is reasonable in LOVECLIM1.2.

Between 130 and 127 ka BP, the different orbital forcing caused a large positive northern hemisphere insolation anomaly, compared to present-day, in late spring and early summer. The maximum top of the atmosphere insolation anomalies during the LIG exceeded 60 Wm⁻² at high northern latitudes in the months May to June while the global annual mean forcing anomaly was as little as 2 Wm⁻² (Berger, 1978). As the GIS has shown to be particularly sensitive to insolation changes in late spring and early summer (Krabill et al., 2004; Otto-Bliesner et al., 2006), it is likely that the early LIG insolation maximum resulted in maximum ablation of the GIS (Otto-Bliesner et al., 2006). This was also found in deep sea geochemical-proxies which indicate large and

LIG climate and Greenland Ice Sheet melting

P. Bakker et al.

Title Page

Abstract

Introduction

Conclusions

References

Tables

Figures



Back

Close

Full Screen / Esc

Printer-friendly Version

Interactive Discussion



steady runoff between 132 and 120 ka BP (Carlson et al., 2008) and a minimal GIS configuration as early as 127 ka BP (Lhomme et al., 2005). We therefore force the LIG climate simulations with orbital and greenhouse-gas concentrations as reconstructed for 130 ka BP (Table 2), in line with the PMIP3 protocol (<http://pmip3.lscce.ipsl.fr/>).

Both our control LIG climate simulation and the pre-industrial (PI; orbital and greenhouse-gas forcing for 1750 AD) were spun up for 3000 yr to ensure quasi-equilibrium conditions in all components of the model, including the deep ocean. The land-sea mask, the GIS topography and albedo were fixed at PI configuration. The fixed land-sea mask will not likely impact the results as the difference in sea level between the two periods is only a couple of meters. From the quasi-equilibrium LIG spin-up simulation, two sets of experiments were performed to investigate the different effects of the partial melting of the GIS: increased runoff, and reduced elevation and extent of the ice sheet. All model simulations have a duration of 500 yr during which the forcings were kept constant. Averages are calculated over the last 100 yr of the simulations.

In the first series of experiments, here called freshwater-forcing (FWF), the 130 ka BP climate was perturbed with a constant runoff flux from the GIS in addition to the runoff already calculated by the model (i.e. the sum of all excess precipitation and snow melt; Opsteegh et al., 1998). The total runoff is evenly distributed over 10 adjacent oceanic grid-cells corresponding to the river outlets of the Greenland landmass (Fig. 1). The FWF-scenarios are based on multiples of the best estimate (0.013 Sv) of Otto-Bliesner et al. (2006) to cover the full range of possible fluxes (Table 1); from 0.5 times up to 23 times 0.013 Sv (0.006.5–0.299 Sv). As all FWF experiments have a duration of 500 yr, the total volume of additional meltwater input to the ocean differs between the simulations, from only ~2 % to up to ~115 % of the total PI volume of the GIS.

To investigate the influence of a lowered topography of the GIS and changes in the extent of the ice sheet, additional experiments have been performed. For three of the FWF experiments, namely 0.013 Sv, 0.052 Sv and 0.143 Sv, the topography of the GIS was lowered in a rudimentary way corresponding to a 30 % decrease of the ice volume. All grid cells of the PI ice sheet, where equally lowered until either bedrock was

LIG climate and Greenland Ice Sheet melting

P. Bakker et al.

Title Page

Abstract

Introduction

Conclusions

References

Tables

Figures

⏪

⏩

◀

▶

Back

Close

Full Screen / Esc

Printer-friendly Version

Interactive Discussion



reached for a particular grid cell or a total volume reduction of 30 % was obtained. The altitude of the bedrock underneath the present-day GIS is deduced from topographic maps provided by the NOAA-database. On the southern tip of Greenland, as well as areas in the northwest and northeast, no ice remained after reducing the volume of the ice sheet. At these ice-free sites a vegetation cover was allowed to develop which results in a strong decrease of the surface albedo. This approach resulted in a configuration of the GIS in broad agreement with reconstructions with a single ice dome over central and northern Greenland, further featuring a lowering of the top of the ice sheet by ~700 m and ice-free conditions over the southern, northwestern and northeastern part of Greenland (Fig. 1). However the reconstructed lowering of the top of the ice sheet is somewhat smaller, between 300 m to 500 m (Otto-Bliesner et al., 2006; Masson-Delmotte et al., 2011). Also, there is still an on-going debate whether or not a southern dome of the GIS remained and finally it has been suggested that the ice sheet was probably steeper as melting concentrated on the fringes (Koerner, 1989; Letréguilly et al., 1991; Cuffey and Marshall, 2000; Lhomme et al., 2005; Otto-Bliesner et al., 2006; Colville et al., 2011). Despite the imperfections in our reconstruction of the LIG GIS, we deem it adequate as more details cannot be provided because of the low resolution of the model. Nonetheless, the simplicity of this approach limits the evaluation of the atmospheric response to changes of the elevation of the GIS.

3 Results and implications

The large number of performed simulations forced with different GIS melt rates provides us with an extensive range of possible climate states: from the warmer than present-day unperturbed 130ka climate state, with a strong overturning circulation, into a situation in which large scale overturning in the North Atlantic is shut down, leading to strong cooling.

LIG climate and Greenland Ice Sheet melting

P. Bakker et al.

Title Page

Abstract

Introduction

Conclusions

References

Tables

Figures



Back

Close

Full Screen / Esc

Printer-friendly Version

Interactive Discussion



3.1 Overturning circulation

The simulated relationship between the FWF and the AMOC strength changes with the size of the FWF (Fig. 2). We take here the maximum strength of the overturning streamfunction in the North Atlantic as a measure for the AMOC strength. The changes in the AMOC strength are strongly related to the combined evolution of deep convection and the sea-ice cover in the two major regions of deep convection in the North Atlantic, the Labrador Sea and the Nordic Seas. The relationship between the AMOC and the FWF is characterized by two shifts, the first between a FWF of 0.039 Sv and 0.052 Sv and the second between 0.13 Sv and 0.143 Sv. In our LIG-ctrl simulation, deep convection takes place in both the Labrador Sea and the Nordic Seas and the simulated AMOC strength of ~ 22 Sv is very similar to the PI strength of ~ 23 Sv. For FWFs between 0.0065 Sv and 0.039 Sv, the strength of the AMOC is reduced by up to 24 % compared to the LIG-ctrl value. In the same range of FWF values, the overturning strength in the Nordic Seas (Fig. 2) does not significantly decrease. For a FWF of 0.52 Sv, the strength of the AMOC is suddenly reduced to a value of ~ 14 Sv, 39 % weaker compared to the LIG-ctrl simulation. The AMOC strength is only slightly reduced for larger FWFs up to 0.117 Sv. Along with the sudden reduction in AMOC strength between a FWF of 0.039 Sv and 0.052 Sv, the maximum sea-ice cover in the Labrador Sea jumps from a cover of around 28 % up to a cover just under 60 % (note that the absolute value of the sea-ice cover strongly depends on the exact definition of the region under consideration). For the same forcings, no significant changes are simulated in both the overturning strength and the maximum sea-ice cover in the Nordic Seas. For FWFs of 0.143 Sv and larger, both the strength of the AMOC as well as the overturning strength and the maximum sea-ice cover in the Nordic Seas depict a clear negative trend towards an AMOC strength of less than 5 Sv and a maximum sea-ice cover of around 100 %. The sea-ice cover in the Labrador Sea does not significantly change for such large FWFs, compared to a FWF of 0.052 Sv.

LIG climate and Greenland Ice Sheet melting

P. Bakker et al.

Title Page

Abstract

Introduction

Conclusions

References

Tables

Figures



Back

Close

Full Screen / Esc

Printer-friendly Version

Interactive Discussion



Because of non-linear processes and feedbacks between the ocean circulation and the sea-ice cover, our simulations result in 3 different climate “regimes” (Fig. 3), differing mainly in the location of the main site(s) of active deep convection. For a FWF between 0 Sv and 0.039 Sv, the reduction in the AMOC strength is mainly due to a reduction in small-scale deep convection in the Irminger Sea (not shown) combined with a first decrease of deep convection in the Labrador Sea in the higher end of this range of FWFs. Overall however, deep convection in this regime, to which we refer as regime 1, takes place in both the Labrador Sea and the Nordic Seas. In both regions the maximum sea-ice cover is still limited. The evolution of deep convection in the Irminger- and Labrador Sea in regime 1, are decoupled from the evolution of deep convection in the Nordic Seas with even a small, though insignificant, increase in the latter. Such an anticorrelation between the major convection sites for moderate freshwater addition was also found by Stouffer et al. (2006). In the second regime, for FWFs between 0.052 Sv and 0.13 Sv, the additional runoff from the GIS has sufficiently decreased the density of the surface waters in the Labrador Sea which, in combination with enhanced sea-ice formation, shuts down deep convection in that region. In regime 2, large-scale deep convection only takes place in the Nordic Seas. The changes from regime 2 into regime 3 are more gradual but still apparent. For a FWF larger than 0.13 Sv, we simulate a third regime in which the overturning strength in the Nordic Seas is significantly weakened and the maximum sea-ice cover in the region starts to increase more rapidly. A shutdown of deep convection and a full sea-ice cover in the Nordic Seas is reached for FWFs over ~ 0.2 Sv. In both regime 2 and 3, the evolution of the overturning strength in the Nordic Seas is again coupled to the evolution of the AMOC strength.

In the remainder of this manuscript, the three regimes will be characterized by the scenarios with a FWF of 0.013 Sv, 0.052 Sv and 0.143 Sv. Despite differences between the simulated climates within one regime, this approach gives a clear picture of the large-scale climatic changes in the North Atlantic region as simulated for increasingly large melt rates of the GIS.

3.2 Characteristics of the surface climate in the three different regimes

In the different LIG climate simulations presented here, the surface climate in the North Atlantic region differs from the PI as a result of both changes in the orbital and greenhouse-gas forcing as well as changes in the melt rate of the GIS. The characteristics of the surface climate are presented by describing both July and January surface air temperature anomalies and yearly averaged sea surface salinity anomalies.

In the LIG-ctrl simulation, the impact of changes in only the orbital and greenhouse gas forcings are visible (Fig. 4). Because of the positive early-LIG northern hemisphere summer insolation anomaly compared to present-day, the LIG-ctrl simulations show a 1°C to 3°C rise in July surface air temperatures over most of the region in comparison with PI, with amplification of the anomalies to over 5 °C over continental areas (Fig. 4). In contrast, as the northern hemisphere winter insolation anomaly is only small, LIG January surface air temperatures are fairly similar to the PI over most of the North Atlantic region. There are however some exceptions, as over the far east of the European continent we simulate a more continental regime which results in a 1°C to 3°C lowering of LIG January surface air temperatures compared to PI. The other exceptions are the high-latitude areas, especially the far north of the Labrador Sea and north of Svalbard, where a reduction in summer sea-ice extent (not shown) strongly affects January surface air temperatures resulting in a warming of 1 to over 5°C compared to the PI. Otto-Bliesner et al. (2006) simulated similar 130 ka BP surface temperatures, providing confidence in our LIG climate simulations without additional GIS melting. The surface salinity in our LIG-ctrl simulation (Fig. 4) differs from the PI only over the Arctic Ocean and along the southern shores of Greenland where a decrease of up to 2 psu (practical salinity units) results from changes in the sea-ice cover and the hydrological cycle (not shown).

Forcing climate with an increased melt rate of the GIS on top of LIG orbital and greenhouse gas forcings, results in very different patterns of surface temperature and sea surface salinity anomalies within the North Atlantic region. Note that, because our

CPD

7, 2763–2801, 2011

LIG climate and Greenland Ice Sheet melting

P. Bakker et al.

Title Page

Abstract

Introduction

Conclusions

References

Tables

Figures

◀

▶

◀

▶

Back

Close

Full Screen / Esc

Printer-friendly Version

Interactive Discussion



surface ocean water around Greenland, it is first advected by the surface currents into the Labrador Sea and then via the southern part of the subpolar gyre to the eastern side of the basin.

3.3 Influence of changes in topography and albedo

5 We have incorporated changes in the extent and elevation of the GIS to study both their direct effect on the LIG climate of the North Atlantic region as well as the impact on the FWF induced changes. Over the ice sheet itself the lower elevation results in a rise of July surface air temperatures of around 2 °C compared to the LIG-ctrl simulation (not corrected for the direct impact of elevation changes) while temperatures over the
10 deglaciated areas rise up to 6 °C because of the lower surface albedo (Fig. 5). These results are similar to findings of Driesschaert et al. (2007) who simulated future GIS melting. The warming over Greenland also partly counteracts the FWF-induced cooling in the Irminger Sea and Labrador Sea.

Lowering the elevation of the GIS also affects the Nordic Seas because of changes
15 in the large-scale atmospheric circulation. Since the GIS is a major obstacle for the circumpolar northern hemisphere Rossby wave – substantially contributing to the pattern of high and low pressure systems over the North Atlantic (Hoskins and Karoly, 1981) – a lower elevation of the GIS induces a distinct pattern of surface pressure anomalies. Similar to what Ridley et al. (2005) found in simulations for a future climate with a completely melted GIS, both the high pressure system located over the
20 southeast of Greenland and the low pressure system over the Norwegian and Barents Seas are weakened (not shown). As further found by Goosse et al. (2002) in a previous version of LOVECLIM, the weakening of the low pressure system over the Norwegian and Barents Seas has a negative impact on the convection strength and therefore on temperatures in the Norwegian and the Barents Seas (cooling of 2 °C to
25 4 °C). As explained by Goosse et al. (2002), the mechanism behind it involves a coupling between the atmosphere, sea-ice and the ocean. Furthermore, our simulations show that the lowering of the elevation of the GIS not only directly reduces the strength

LIG climate and Greenland Ice Sheet melting

P. Bakker et al.

Title Page

Abstract

Introduction

Conclusions

References

Tables

Figures



Back

Close

Full Screen / Esc

Printer-friendly Version

Interactive Discussion



of the overturning in the Nordic Seas, it also enhances the sensitivity of the Nordic Seas overturning strength to the FWF (Fig. 2). Our simulations suggest that the overall AMOC strength modulates the decadal variability of the northern hemisphere sea-ice volume described by Goosse et al. (2002). Therefore, as the result of a weakening AMOC, the climate resides more and more in one state of the decadal variability – lower atmospheric temperatures in the Arctic, increased sea-ice volume, and reduced overturning in the Nordic Seas – (results not shown here). In regime 3, the combination of the direct impact of the lowering of the topography of the GIS on the overturning in the Nordic Seas and the positive feedback to the FWF, results in a further 14 % decrease of the AMOC strength in addition to the FWF induced changes (Fig. 2).

Incorporating changes in the elevation and extent of the GIS in the simulations provides a first insight into its impact on Greenland temperatures, the impact on the climate in the Nordic Seas and the relationship between the decadal variability of the northern hemisphere sea-ice volume and the FWF. However, in particular the latter relationship requires a more thorough investigation which is beyond the scope of this study.

3.4 The significant impact on July surface air temperatures of GIS melting

If a climate signal at a certain location is to be preserved in the geological archive, the magnitude of the signal has to be significantly larger than the internal variability on timescales of decades and larger (depending on the resolution of the climate archive). It is only for these locations that conclusions can be drawn during the upcoming model-data comparison. We therefore investigate for which locations the simulated impact on July surface air temperatures is significant compared to the unforced, multi-decadal climate variability in the LIG-ctrl simulation (Fig. 6). The investigated forcings are the FWF (for the three different regimes), the changes in extent and elevation of the GIS, and the three forcings combined.

The analysis shows that the impact of the FWF in regime 1 is small and no area is significantly influenced. However, the changes in the topography and albedo do significantly alter July surface air temperatures, mainly over the GIS itself, parts of

LIG climate and Greenland Ice Sheet melting

P. Bakker et al.

Title Page

Abstract

Introduction

Conclusions

References

Tables

Figures



Back

Close

Full Screen / Esc

Printer-friendly Version

Interactive Discussion



the Labrador Sea, and the ocean roughly between northern Greenland and Svalbard (orange in Fig. 6). In regime 2 a significantly large impact of the FWF is simulated, mainly over the Labrador Sea, parts of the North Atlantic Ocean (between 35° N and 55° N), the ocean between northern Greenland and Svalbard, large parts of the Nordic Seas, parts of the UK and the Iberian Peninsula (red and yellow in Fig. 6). The impact of the lowering of the elevation and the reduced extent of the GIS is simulation over the same region (red in Fig. 6) although now the GIS is also affected (orange in Fig. 6) while the impact is no longer significant over the ocean between northern Greenland and Svalbard (yellow in Fig. 6). The latter implies that the temperature changes over that area resulting from both the FWF in regime 2 and from the changes in elevation and extent of the GIS, cancel each other out. Interestingly, over the Irminger Sea the unforced, multi-decadal climate variability is still larger than the substantial FWF-forced temperature anomaly in that region. In regime 3 a significant impact of the FWF is simulated for almost the entire North Atlantic region, except for the northern part of Greenland and over Eastern Europe, where the impact is only significant if the changes in the topography and extent of the GIS are included.

Describing the regions where the climatic impact of a melting GIS is likely to be detected in this way, does not account for uncertainties in the temperature reconstructions nor simulated temperature biases. It can therefore not be concluded that the changes should show up in reconstructions, since the temperature change might still be too small despite being statistically significant in our simulations. However, in regions where no significant GIS melting impact is simulated, it appears unlikely to be registered in proxy-based temperature reconstructions.

Combining the results on the impact and the significance of the changes in July surface air temperatures, we obtain distinct geographic patterns showing the influence of different melt rates of the GIS on the LIG climate in the North Atlantic region. In regime 1 there are no regions where July surface air temperatures are significantly altered. A $\sim 6^{\circ}\text{C}$ cooling compared to the LIG-ctrl simulation is however simulated over the Labrador Sea in regime 2 (see also Fig. 7) together with a cooling of around $\sim 2^{\circ}\text{C}$

LIG climate and Greenland Ice Sheet melting

P. Bakker et al.

Title Page

Abstract

Introduction

Conclusions

References

Tables

Figures



Back

Close

Full Screen / Esc

Printer-friendly Version

Interactive Discussion



over the southeast of Baffin Island and the North Atlantic Ocean between 35° N and 55° N. On top of these changes, regime 3 is characterized by a ~2°C cooling in the Nordic Seas and over Scandinavia.

If the impact of lowered topography and decreased extent of the GIS are included, the results show different geographic patterns of temperature anomalies for specific regions compared to simulations only forced with enhanced GIS melting. Including these forcings, a significant July surface air temperature increases of around 2°C is simulated in all three regimes over the central GIS and a 6°C increase over the deglaciated areas. With respect to the LIG-ctrl simulation, we simulate a 2°C to 4°C warming of parts of the northern Labrador Sea in regime 1, which is however no longer present under the influence of larger FWFs. Thus, if topography and albedo changes are included, we simulate different temperature anomalies over the GIS and the adjacent coastal waters. However the main geographic patterns of temperature anomalies forced by GIS melting remain unaltered.

3.5 Constraints on LIG melt rate of the GIS

In order to constrain the range of possible melt rates of the GIS during the LIG, we will compare the simulated deep ocean circulation in the three regimes with proxy-based reconstructions.

Based on reconstructions of the vertical stratification of the water column in the Labrador Sea, Hillaire-Marcel et al. (2001) concluded that no LSW was formed during the LIG. Rasmussen et al. (2003) however contradicted this view. Using benthic $\delta^{13}\text{C}$ reconstructions, they concluded that during Termination 2 and the early LIG, a weakly ventilated, LSW-like water mass should have been present at intermediate depth in the Labrador Sea region. However, it was possibly formed outside of the Labrador Sea and flowed in from the east. For the later part of the LIG, they reconstructed Labrador Sea surface and bottom water conditions comparable to modern day conditions. Different reconstructions of LSW formation during the LIG also result from studies on sediment cores recovered just outside of the Labrador Sea. They show that LSW formation was

LIG climate and Greenland Ice Sheet melting

P. Bakker et al.

Title Page

Abstract

Introduction

Conclusions

References

Tables

Figures



Back

Close

Full Screen / Esc

Printer-friendly Version

Interactive Discussion



either weaker and occurring at shallower depth, or that it was absent altogether (Evans et al., 2007; Hodell et al., 2009). Although the characteristics of the ocean circulation in the Labrador Sea during the LIG remain unresolved, these proxy-based studies suggest that LSW formation was weak or absent during the early LIG, ruling out the oceanographic situation found in regime 1.

LIG deep ocean circulation in the Nordic Seas is also under debate. There are opposing views on the timing of the maximum overturning strength, either coinciding with the insolation optimum (Cortijo et al., 1994, 1999) or occurring during a later part of the interglacial (Rasmussen et al., 2003; Bauch and Erlenkeuser, 2008; Nieuwenhove et al., 2008, 2011). Although our simulations suggest that melting of the GIS could have affected the overturning circulation in the Nordic Seas, possibly delaying maximum strength until after the insolation optimum, a very large melt rate of over 0.143 Sv is needed. As such a flux is at the very high end of the range of reconstructed FWF, we conclude that it is not likely that GIS melting strongly reduced deep water formation in the Nordic Seas during the LIG. Assuming that the AMOC in our model has a reasonable sensitivity to FWF, our results suggest therefore that the most likely climate state is regime 2 with an average GIS melt rate between 0.052 Sv and 0.13 Sv.

3.6 Impact of GIS melting on LIG climate

The most likely state of the LIG climate under the influence of a partial melting of the GIS is, in our simulations, characterized by significant surface temperature anomalies in specific regions. Comparing these anomaly patterns with temperature reconstructions, can help us understand the impact of a melting GIS on the LIG climate.

The most comprehensive compilation of climate reconstructions for the LIG to date was presented by the CAPE-members (2006). They mapped maximum LIG Arctic summer temperature anomalies based on a range of different terrestrial, oceanic and ice core related proxies. To circumvent large uncertainties in dating geological records from the LIG, the data compilation does not represent temperature reconstructions of a specific age but rather maps the maximum LIG summer temperatures for all the

LIG climate and Greenland Ice Sheet melting

P. Bakker et al.

Title Page

Abstract

Introduction

Conclusions

References

Tables

Figures



Back

Close

Full Screen / Esc

Printer-friendly Version

Interactive Discussion



different sites. We have extended the model-data comparison with maximum LIG summer temperature reconstructions from the Iberian coastal waters (Sánchez Goñi et al., 2008) and the Labrador Sea (Hillaire-Marcel et al., 2001) for a better spatial coverage of the North Atlantic region. However, we restrict our model-data comparison to those regions in which significant impact of a melting GIS was simulated (Figure 6). We use July surface air temperatures on land and August sea surface temperature for marine sites, corresponding to the warmest months.

For all continental sites, the simulations are within the range of the reconstructed temperatures except on the southern part of Baffin Island and the site just south of the Barents Sea (Fig. 7). By contrast, the comparison for marine sites shows a more complex spatial pattern. For most of the Norwegian Sea and for the central and eastern North Atlantic Ocean, the simulated temperatures are in agreement with the reconstructions. However, over the Labrador Sea, reconstructions show $\sim 5^{\circ}\text{C}$ higher summer sea surface temperatures, in stark contrast to a simulated cooling of 3°C compared to the PI. Smaller differences between simulated and reconstructed temperatures are found in the Irminger Sea, parts of the Norwegian Sea and in the Barents Sea.

The model-data comparison reveals an apparent geographical pattern: good correspondence over the central- and eastern part of the North Atlantic and a mismatch over the Labrador Sea, the Irminger Sea and southern Baffin Island. This pattern matches the simulated climatic impact on July surface air temperatures in regime 2. This would imply that, if during the early LIG insolation maximum GIS melting forced the climate into regime 2, reconstructed LIG maximum summer temperatures in the Labrador Sea, the Irminger Sea and over southern Baffin Island were reached during a later part of the LIG. A delayed thermal maximum relative to the insolation maximum has also been suggested by (Renssen et al., 2009) for the early Holocene, during which the climate was forced by melting of the Laurentide Ice Sheet. Also for parts of the Norwegian and Barents Seas region, modelled summer surface temperatures are not in agreement with reconstructions. This could suggest that this area was also impacted by GIS melting, however the model-data comparison is ambiguous. Interestingly, our

LIG climate and Greenland Ice Sheet melting

P. Bakker et al.

Title Page

Abstract

Introduction

Conclusions

References

Tables

Figures



Back

Close

Full Screen / Esc

Printer-friendly Version

Interactive Discussion



simulations suggest that the influence of GIS melting on the Norwegian and Barents Seas region is not solely the result of the freshwater flux but of both the freshwater flux and the atmospheric response to the reduced elevation and extent of the GIS.

4 Discussion

4.1 LIG and future melt rates of the GIS

The most likely rates of GIS melting during the LIG (between 0.052 Sv and 0.13 Sv) inferred from our simulations, are significantly larger than the rates which can be inferred from different proxy- and modelling-based studies (up to 0.013 Sv). However, as these studies present average values over the whole LIG, melt rates might have been significantly larger during shorter periods of time, possibly a couple of hundreds of years. This is quite likely as for several periods of around 400 years, maximum rates of global sea-level change, including an important though uncertain contribution of the GIS, of up to 0.29 Sv have been reconstructed for the LIG (Rohling et al., 2008). The range of LIG GIS melt rates found in this study is also very similar to predictions of future GIS melting. Forcing LOVECLIM, coupled to an active ice-sheet model, with increased greenhouse gas concentrations (IPCC SRES A2-scenario), Driesschaert et al. (2007) simulate freshwater fluxes from the GIS evolving from around 0.03 Sv up to 0.08 Sv in the course of several centuries. Based on the extrapolation of GIS mass loss measurements, Rignot et al. (2011) estimated an average freshwater flux of 0.033 ± 0.013 Sv until the year 2100. If the simulated sensitivity of the North Atlantic climate for the LIG is extrapolated into the future, we find that, in line with Driesschaert et al. (2007), these meltwater fluxes will not be sufficient to shut down the AMOC, nor will they substantially cool climate in Europe. The estimated future GIS melt fluxes are however similar to the fluxes for which we simulated a significant impact on deep convection in the Labrador Sea.

LIG climate and Greenland Ice Sheet melting

P. Bakker et al.

Title Page

Abstract

Introduction

Conclusions

References

Tables

Figures



Back

Close

Full Screen / Esc

Printer-friendly Version

Interactive Discussion



4.2 Other mechanisms preventing LSW formation

GIS melting is a likely candidate to have inhibited deep convection in the Labrador Sea during the early LIG. However, it cannot be ruled out that an alternative mechanism prevented deep convection in the Labrador Sea. An alternative mechanism explaining the reconstructed climate state could be increased transport and melt of Arctic sea-ice which could have freshened the East- and West Greenland Current. Furthermore, part of the sea-level high stand during the LIG has been attributed to partial melting of the West Antarctic Ice Sheet (e.g. Overpeck et al., 2006). This freshwater input and its effect on the climate are still poorly understood but it might weaken the AMOC (Swingedouw et al., 2009) and therewith provide an alternative mechanism for the reconstructed changes in the LIG climate of the North Atlantic region.

4.3 Assessing model uncertainties

Although climate models offer a very useful tool to investigate past climate variability, findings about the simulated stability of the climate to certain perturbations depend heavily on uncertainties in the physics, parameter-set (tuning) and applied forcing scenario. Here we discuss the performance of our LOVECLIM simulations with respect to the most important uncertainties.

As shown by Stouffer et al. (2006) the LOVECLIM EMIC performs rather well compared to GCMs in describing the relationship between FWFs and the overturning strength in the North Atlantic. However, they also show that the models differ a lot when it comes to describing the exact location and sensitivity of the deep convection site in the Labrador Sea. So, although LOVECLIM simulates deep convection in the right region under present-day forcings, deep convection changes in the Labrador Sea region should be interpreted with care.

Aside from model-dependent climate sensitivity, a second major source of uncertainties is related to the applied forcing scenario. The scenarios were set up as equilibrium experiments forced with 130 ka orbital configuration and greenhouse gas

LIG climate and Greenland Ice Sheet melting

P. Bakker et al.

Title Page

Abstract

Introduction

Conclusions

References

Tables

Figures

⏪

⏩

◀

▶

Back

Close

Full Screen / Esc

Printer-friendly Version

Interactive Discussion



concentrations, and with a combination of changes in the GIS elevation, extent and meltwater flux. The choice of 130 ka BP forcings is somewhat arbitrary as the timing of the period of enhanced GIS melt during the LIG is uncertain. The orbital and greenhouse gas forcings do not differ largely within the early LIG and timing of their changes is (relatively) well constrained. However, small differences might cause the climate to cross a threshold and therewith potentially have large implications on the described results. Further, simulations with a reduction in GIS elevation and extent suggest a strong response in the regional atmospheric circulation. However, despite that similar effects on the atmospheric circulation were found in other studies (e.g. Lunt et al., 2004; Vizcaíno et al., 2008), corroborating our findings, models containing a more detailed and realistic representation of the atmospheric physics and dynamics are better suited for further in-depth research into this process. Nevertheless, by performing a range of sensitivity experiments, we systematically dealt with the uncertainty in GIS-melt forcing of the model. Finally, three major assumptions are made in the experimental setup of the scenarios. First, simulations start from a climate characterized by deep water formation in both the Nordic and Labrador Seas. It is however possible that deep convection did not occur on a sustained basis in these regions during the early LIG (Hillaire-Marcel et al., 2001) because it was inhibited by the meltwater release during the preceding deglaciation up to that time. However, this would not exclude melting of the GIS as an important mechanism which inhibited deep convection after the deglaciation. Secondly, a constant FWF is prescribed in our simulations, however short periods of high meltwater production could have had a profound and lasting influence on the ocean dynamics. A third assumption pertains to the constant, PI configuration of all global ice sheets except the GIS. From sea level reconstructions, it has been assumed that the major ice sheets had already melted away at the beginning of the LIG and that sea level was at most a couple of meters below its high stand. However, this does not rule out the possibility that some glacial ice remained, providing meltwater to different parts of the world's oceans like the Southern Ocean or the Norwegian and Barents Seas. As the focus of this study is on the impact of the GIS melting, we have adopted

LIG climate and Greenland Ice Sheet melting

P. Bakker et al.

Title Page

Abstract

Introduction

Conclusions

References

Tables

Figures



Back

Close

Full Screen / Esc

Printer-friendly Version

Interactive Discussion



the assumption that the configuration and meltwater input into the ocean of other ice sheets was similar to present-day.

4.4 Outlook

LIG climate was not in equilibrium at the moment GIS melting commenced. Rather the time varying orbital and greenhouse gas forcings led to transient climatic changes. Performing transient simulations including a range of GIS melting scenarios may provide valuable insight into additional feedbacks and into the importance of the timing and duration of GIS melting. Future research will be dedicated to this and will complement the results described here. Further research into this subject will also be on including the carbon cycle in the simulations to provide a more direct comparison with proxy-based reconstructions of the past overturning circulation.

5 Conclusions

We have tested the models sensitivity to GIS melting and our main findings are:

- For enhanced melting of the GIS we find a nonlinear relationship between the AMOC, deep convection in the Labrador Sea and deep convection in the Nordic Seas. For a GIS melt flux smaller than 0.052 Sv, the evolution of deep convection in the Nordic Seas is decoupled from the evolution of the AMOC while for larger GIS melt rates their evolution is again synchronous.
- For additional GIS melt fluxes below 0.052 Sv, we find little impact on climate in the North Atlantic region. Deep convection takes place in both the Labrador Sea and the Nordic Seas and no significant changes in July surface air temperatures are simulated.
- For additional GIS melt fluxes of between 0.052 Sv and 0.13 Sv, deep convection is inhibited in the Labrador Sea while in the Nordic Seas deep convection remains

LIG climate and Greenland Ice Sheet melting

P. Bakker et al.

Title Page

Abstract

Introduction

Conclusions

References

Tables

Figures



Back

Close

Full Screen / Esc

Printer-friendly Version

Interactive Discussion



LIG climate and Greenland Ice Sheet melting

P. Bakker et al.

Title Page

Abstract

Introduction

Conclusions

References

Tables

Figures



Back

Close

Full Screen / Esc

Printer-friendly Version

Interactive Discussion



unaffected. July surface air temperatures decrease by as much as 6°C over the Labrador Sea and by around 2°C over the southern part of Baffin Island and part the North Atlantic Ocean, roughly between 40° N and 60° N.

- For additional GIS melt fluxes of between 0.052 Sv and 0.13 Sv, deep convection is inhibited in the Labrador Sea while in the Nordic Seas deep convection remains unaffected. July surface air temperatures decrease by as much as 6°C over the Labrador Sea and by around 2°C over the southern part of Baffin Island and part the North Atlantic Ocean, roughly between 40°n and 60° N.
- For additional GIS melt fluxes of 0.143 Sv and larger, we find that the strength of the overturning in the Nordic Seas is weakened. July surface air temperatures decrease by around 2°C over the Norwegian and Barents Seas, over Scandinavia and over the Iberian Peninsula.
- Over large parts of Central and Eastern Europe we simulate no changes in July surface air temperatures in neither of these regimes.
- In a series of idealized simulations we show that a decreased altitude and extent of the GIS results in a 2°C rise of July surface air temperatures over the centre of the GIS and a 6°C rise over the deglaciated areas. Furthermore, the lower elevation of the GIS increases the sensitivity of the overturning strength in the Nordic Seas to enhanced melting of the GIS.
- We have constrained a likely – though model-specific – range of LIG GIS melt rates to 0.052 Sv to 0.13 Sv by selecting the climate regime for which the configuration of the North Atlantic Ocean circulation is most consistent with proxy-based reconstructions for the LIG.
- By comparing the simulated July surface air temperatures for this regime (GIS melt rates between 0.052 Sv and 0.13 Sv) with reconstructed maximum LIG summer temperatures, we show that melting of the GIS possibly delayed the LIG

thermal maximum in the western part of the North Atlantic region relative to the insolation maximum and inhibited the formation of Labrador Sea Water.

Acknowledgements. The research leading to these results has received funding from the European Union's Seventh Framework programme (FP7/2007-2013) under grant agreement no° 243908, "Past4Future. Climate change – Learning from the past climate."

References

- Alley, R. B., Andrews, J. T., Brigham-Grette, J., Clarke, G. K. C., Cuffey, K. M., Fitzpatrick, J. J., Funder, S., Marshall, S. J., Miller, G. H., Mitrovica, J. X., Muhs, D. R., Otto-Bliesner, B. L., Polyak, L., and White, J. W. C.: History of the Greenland Ice Sheet: paleoclimatic insights, *Quaternary Sci. Rev.*, 29, 1728–1756, 2010. 2765, 2767
- Bacon, S., Gould, W. J., and Jia, Y.: Open-ocean convection in the Irminger Sea, *Geophys. Res. Lett.*, 30, 1246, 2003. 2765
- Barber, D., Dyke, A., Hillaire-Marcel, C., Jennings, A., Andrews, J. T., Kerwin, M., Bilodeau, G., McNeely, R., Southon, J., Morehead, M., and Gagnon, J.: Forcing of the cold event of 8.200 years ago by catastrophic drainage of Laurentide lakes, *Nature*, 400, 344–348, 1999. 2766
- Bauch, H. A. and Erlenkeuser, H.: A "critical" climatic evaluation of last interglacial (MIS 5e) records from the Norwegian Sea, *Polar Research*, 27, 135–151, 2008. 2767, 2780
- Berger, A. L.: Long-term variations of caloric insolation resulting from the earth's orbital elements, *Quaternary Res.*, 9, 139–167, 1978. 2769
- Broecker, W. S., Bond, G., Klas, M., Bonani, G., and Wolfli, W.: A Salt Oscillator in the Glacial Atlantic? 1. The Concept, *Paleoceanography*, 5, 469–477, 1990. 2765
- Brovkin, V., Bendtsen, J., Claussen, M., Ganopolski, A., Kubatzki, C., Petoukhov, V., and Andreev, A.: Carbon cycle, vegetation, and climate dynamics in the Holocene: Experiments with the CLIMBER-2 model, *Global Biogeochem. Cy.*, 16, 1139, doi:10.1029/2001GB001662, 2002. 2768
- CAPE-members: Last Interglacial Arctic warmth confirms polar amplification of climate change, *Quaternary Sci. Rev.*, 25, 1383–1400, 2006. 2765, 2780, 2801
- Carlson, A. E., Stoner, J. S., Donnelly, J. P., and Hillaire-Marcel, C.: Response of the southern Greenland Ice Sheet during the last two deglaciations, *Geology*, 36, 359–362, 2008. 2767, 2770, 2793

LIG climate and Greenland Ice Sheet melting

P. Bakker et al.

Title Page

Abstract

Introduction

Conclusions

References

Tables

Figures



Back

Close

Full Screen / Esc

Printer-friendly Version

Interactive Discussion



LIG climate and Greenland Ice Sheet melting

P. Bakker et al.

Title Page

Abstract

Introduction

Conclusions

References

Tables

Figures

◀

▶

◀

▶

Back

Close

Full Screen / Esc

Printer-friendly Version

Interactive Discussion



Chen, J. H., Curran, H. A., White, B., and Wasserburg, G. J.: Precise chronology of the last interglacial period: 234U-230Th data from fossil coral reefs in the Bahamas, *Geol. Soc. Am. Bull.*, 103, 82–97, 1991. 2767

Colville, E. J., Carlson, A. E., Beard, B. L., Hatfield, R. G., Stoner, J. S., Reyes, A. V., and Ullman, D. J.: Sr-Nd-Pb Isotope Evidence for Ice-Sheet Presence on Southern Greenland During the Last Interglacial, *Science*, 333, 620–623, 2011. 2767, 2771, 2793

Cortijo, E., Duplessy, J. C., Labeyrie, L., Leclair, H., Duprat, J., and van Weering, T. C. E.: Eemian cooling in the Norwegian Sea and North Atlantic ocean preceding continental ice-sheet growth, *Nature*, 372, 446–449, 1994. 2766, 2780

Cortijo, E., Lehman, S., Keigwin, L., Chapman, M., Paillard, D., and Labeyrie, L.: Changes in Meridional Temperature and Salinity Gradients in the North Atlantic Ocean (30°–72° N) during the Last Interglacial Period, *Paleoceanography*, 14, 23–33, 1999. 2767, 2780

Cuffey, K. M. and Marshall, S. J.: Substantial contribution to sea-level rise during the last interglacial from the Greenland ice sheet, *Nature*, 404, 591–594, 2000. 2767, 2771, 2793

Driesschaert, E., Fichefet, T., Goosse, H., Huybrechts, P., Janssens, I., Mouchet, A., Munhoven, G., Brovkin, V., and Weber, S. L.: Modeling the influence of Greenland ice sheet melting on the Atlantic meridional overturning circulation during the next millennia, *Geophys. Res. Lett.*, 34, L10707, doi:10.1029/2007GL029516, 2007. 2764, 2766, 2776, 2782

Evans, H. K., Hall, I. R., Bianchi, G. G., and Oppo, D. W.: Intermediate water links to Deep Western Boundary Current variability in the subtropical NW Atlantic during marine isotope stages 5 and 4, *Paleoceanography*, 22, PA3209, doi:10.1029/2006PA001409, 2007. 2767, 2780

Goosse, Selten, Haarsma, and Opsteegh: A mechanism of decadal variability of the sea-ice volume in the Northern Hemisphere, *Clim. Dynam.*, 19, 61–83, 2002. 2776, 2777

Goosse, H. and Fichefet, T.: Importance of ice-ocean interactions for the global ocean circulation: A model study, *J. Geophys. Res.*, 104, 23337–23355, 1999. 2768

Goosse, H., Brovkin, V., Fichefet, T., Haarsma, R. J., Huybrechts, P., Jongma, J. I., Mouchet, A., Selten, F. M., Barriat, P., Campin, J., Renssen, H., Roche, D. M., Timmermann, A., and Opsteegh, J. D.: Description of the Earth system model of intermediate complexity LOVECLIM version 1.2, *Geoscientific Model Development*, 3, 309–390, 2010. 2768, 2769

Heinrich, H.: Origin and consequences of cyclic ice rafting in the northeast Atlantic Ocean during the past 130 000 years, *Quat. Res.*, 29, 143–152, 1988.

Hillaire-Marcel, C., de Vernal, A., Bilodeau, G., and Weaver, A. J.: Absence of deep-water

LIG climate and Greenland Ice Sheet melting

P. Bakker et al.

Title Page

Abstract

Introduction

Conclusions

References

Tables

Figures

◀

▶

◀

▶

Back

Close

Full Screen / Esc

Printer-friendly Version

Interactive Discussion



formation in the Labrador Sea during the last interglacial period, *Nature*, 410, 1073–1077, 2001. 2767, 2779, 2781, 2784, 2801

Hodell, D. A., Minth, E. K., Curtis, J. H., McCave, I. N., Hall, I. R., Channell, J. E. T., and Xuan, C.: Surface and deep-water hydrography on Gardar Drift (Iceland Basin) during the last interglacial period, *Earth Planet. Sci. Lett.*, 288, 10–19, 2009. 2767, 2780

Hofmann, M. and Rahmstorf, S.: On the stability of the Atlantic meridional overturning circulation, *Proceedings of the National Academy of Sciences*, 106, 20584–20589, 2009. 2766

Hoskins, B. J. and Karoly, D. J.: The Steady Linear Response of a Spherical Atmosphere to Thermal and Orographic Forcing, *J. Atmos. Sci.*, 38, 1179–1196, 1981. 2776

Israelson, C. and Wohlfarth, B.: Timing of the Last-Interglacial High Sea Level on the Seychelles Islands, *Indian Ocean, Quaternary Res.*, 51, 306–316, 1999. 2767

Koerner, R. M.: Ice Core Evidence for Extensive Melting of the Greenland Ice Sheet in the Last Interglacial, *Science*, 244, 964–968, 1989. 2771

Krabill, W., Hanna, E., Huybrechts, P., Abdalati, W., Cappelen, J., Csatho, B., Frederick, E., Manizade, S., Martin, C., Sonntag, J., Swift, R., Thomas, R., and Yungel, J.: Greenland Ice Sheet: Increased coastal thinning, *Geophys. Res. Lett.*, 31, L24402, doi:10.1029/2004GL021533, 2004. 2769

Kuhlbrodt, T., Griesel, A., Montoya, M., Levermann, A., Hofmann, M., and Rahmstorf, S.: On the driving processes of the Atlantic meridional overturning circulation, *Rev. Geophys.*, 45, RG2001, doi:10.1029/2004RG000166, 2007. 2765

Letréguilly, A., Huybrechts, P., and Reeh, N.: Steady-state characteristics of the Greenland ice sheet under different climates, *J. Glaciol.*, 29, 149–157, 1991. 2771

Lhomme, N., Clarke, G. K. C., and Marshall, S. J.: Tracer transport in the Greenland Ice Sheet: constraints on ice cores and glacial history, *Quaternary Sci. Rev.*, 24, 173–194, 2005. 2767, 2770, 2771, 2793

Lunt, D. J., de Noblet-Ducoudré, N., and Charbit, S.: Effects of a melted greenland ice sheet on climate, vegetation, and the cryosphere, *Climate Dynamics*, 23, 679–694, 2004. 2784

Masson-Delmotte, V., Braconnot, P., Hoffmann, G., Jouzel, J., Kageyama, M., Landais, A., Lejeune, Q., Risi, C., Sime, L., Sjolte, J., Swingedouw, D., and Vinther, B.: Sensitivity of interglacial Greenland temperature and $\delta^{18}\text{O}$ to orbital and CO_2 forcing: climate simulations and ice core data, *Clim. Past Discuss.*, 7, 1585–1630, doi:10.5194/cpd-7-1585-2011, 2011. 2771

McCulloch, M. T. and Esat, T.: The coral record of last interglacial sea levels and sea surface

**LIG climate and
Greenland Ice Sheet
melting**

P. Bakker et al.

Title Page

Abstract

Introduction

Conclusions

References

Tables

Figures



Back

Close

Full Screen / Esc

Printer-friendly Version

Interactive Discussion



temperatures, *Chem. Geol.*, 169, 107–129, 2000. 2767

Muhs, D. R., Simmons, K. R., and Steinke, B.: Timing and warmth of the Last Interglacial period: new U-series evidence from Hawaii and Bermuda and a new fossil compilation for North America, *Quaternary Sci. Rev.*, 21, 1355–1383, 2002. 2767

5 Nieuwenhove, N., Bauch, H. A., Eynaud, F., Kandiano, E., Cortijo, E., and Turon, J.-L.: Evidence for delayed poleward expansion of North Atlantic surface waters during the last interglacial (MIS 5e), *Quaternary Sci. Rev.*, 30, 934–946, 2011. 2767, 2780

Nieuwenhove, v. N., Bauch, H. A., and Matthiessen, J.: Last interglacial surface water conditions in the eastern Nordic Seas inferred from dinocyst and foraminiferal assemblages, *Marine Micropaleontology*, 66, 247–263, 2008. 2767, 2780

10 Opsteegh, J. D., Haarsma, R. J., Selten, F. M., and Kattenberg, A.: ECBILT: a dynamic alternative to mixed boundary conditions in ocean models, *Tellus A*, 50, 348–367, 1998. 2768, 2770

15 Otto-Bliesner, B. L., Brady, E. C., Clauzet, G., Tomas, R., Levis, S., and Kothavala, Z.: Last Glacial Maximum and Holocene Climate in CCSM3, *J. Climate*, 19, 2526–2544, 2006. 2766, 2767, 2769, 2770, 2771, 2774, 2793

Overpeck, J. T., Otto-Bliesner, B. L., Miller, G. H., Muhs, D. R., Alley, R. B., and Kiehl, J. T.: Paleoclimatic Evidence for Future Ice-Sheet Instability and Rapid Sea-Level Rise, *Science*, 311, 1747–1750, 2006. 2783

20 Rahmstorf, S.: Bifurcation of the Atlantic thermohaline circulation in response to changes in the hydrological cycle, *Nature*, 378, 145–149, 1995. 2765

Rahmstorf, S., Crucifix, M., Ganopolski, A., Goosse, H., Kamenkovich, I., Knutti, R., Lohmann, G., Marsh, R., Mysak, L. A., Wang, Z., and Weaver, A. J.: Thermohaline circulation hysteresis: A model intercomparison, *Geophys. Res. Lett.*, 32, L23605, doi:10.1029/2005GL023655, 2005. 2765, 2767, 2769

25 Rasmussen, T. L., Oppo, D. W., Thomsen, E., and Lehman, S. J.: Deep sea records from the southeast Labrador Sea: Ocean circulation changes and ice-rafting events during the last 160,000 years, *Paleoceanography*, 18, 1018, doi:10.1029/2001PA000736, 2003. 2767, 2779, 2780

30 Renssen, H., Goosse, H., Fichefet, T., Campin, J., and M: The 8.2 kyr BP event simulated by a Global Atmosphere-Sea-Ice-Ocean Model, *Geophys. Res. Lett.*, 28, 1567–1570, 2001. 2766, 2767

Renssen, H., Seppa, H., Heiri, O., Roche, D. M., Goosse, H., and Fichefet, T.: The spatial and

LIG climate and Greenland Ice Sheet melting

P. Bakker et al.

Title Page

Abstract

Introduction

Conclusions

References

Tables

Figures

◀

▶

◀

▶

Back

Close

Full Screen / Esc

Printer-friendly Version

Interactive Discussion



temporal complexity of the Holocene thermal maximum, *Nature Geosci.*, 2, 411–414, 2009. 2769, 2781

Ridley, J. K., Huybrechts, P., Gregory, J. M., and Lowe, J. A.: Elimination of the Greenland Ice Sheet in a High CO₂ Climate, *J. Climate*, 18, 3409–3427, 2005. 2766, 2776

5 Rignot, E., Velicogna, I., van den Broeke, M. R., Monaghan, A., and Lenaerts, J.: Acceleration of the contribution of the Greenland and Antarctic ice sheets to sea level rise, *Geophys. Res. Lett.*, 38, L05503, doi:10.1029/2011GL046583, 2011. 2764, 2782

Roche, D. M., Wiersma, A. P., and Renssen, H.: A systematic study of the impact of freshwater pulses with respect to different geographic locations, *Clim. Dynam.*, 34, 997–1013, 2010. 2766

10 Rohling, E., Grant, K., Hemleben, C., Siddal, M., Hoogakker, B., Bolshaw, M., and Kucera, M.: High rates of sea-level rise during the last interglacial period, *Nat. Geosci.*, 1, 38–42, 2008. 2767, 2782

Sánchez Goñi, M. F., Landais, A., Fletcher, W. J., Naughton, F., Desprat, S., and Duprat, J.: Contrasting impacts of Dansgaard-Oeschger events over a western European latitudinal transect modulated by orbital parameters, *Quaternary Sci. Rev.*, 27, 1136–1151, 2008. 2781, 2801

Schmitz, W. J.: On the interbasin-scale thermohaline circulation, *Rev. Geophys.*, 33, 151–173, 1995. 2765

20 Smith, R. S. and Gregory, J. M.: A study of the sensitivity of ocean overturning circulation and climate to freshwater input in different regions of the North Atlantic, *Geophys. Res. Lett.*, 36, L15701, doi:10.1029/2009GL038607, 2009. 2766

Solomon, S., Qin, D., Manning, M., Chen, Z., Marquis, M., Averyt, K., Tignor, M., and Miller, H.: IPCC, 2007: Climate Change 2007: The Physical Science Basis. Contribution of Working Group I to the Fourth Assessment Report of the Intergovernmental Panel on Climate Change, Cambridge University Press, Cambridge, United Kingdom and New York, NY, USA,, p. 996, 2007. 2764, 2766

25 Stirling, C. H., Esat, T. M., McCulloch, M. T., and Lambeck, K.: High-precision U-series dating of corals from Western Australia and implications for the timing and duration of the Last Interglacial, *Earth Planet. Sci. Lett.*, 135, 115–130, 1995. 2767

30 Stirling, C. H., Esat, T. M., Lambeck, K., and McCulloch, M. T.: Timing and duration of the Last Interglacial: evidence for a restricted interval of widespread coral reef growth, *Earth Planet. Sci. Lett.*, 160, 745–762, 1998. 2767

- Stommel, H.: Thermohaline Convection with Two Stable Regimes of Flow, *Tellus*, 13, 224–230, 1961. 2765
- Stouffer, R. J., Yin, J., Gregory, J. M., Dixon, K. W., Spelman, M. J., Hurlin, W., Weaver, A. J., Eby, M., Flato, G. M., Hasumi, H., Hu, A., Jungclaus, J. H., Kamenkovich, I. V., Levermann, A., Montoya, M., Murakami, S., Nawrath, S., Oka, A., Peltier, W. R., Robitaille, D. Y., Sokolov, A., Vettoretti, G., and Weber, S. L.: Investigating the Causes of the Response of the Thermohaline Circulation to Past and Future Climate Changes, *J. Climate*, 19, 1365–1387, 2006. 2773, 2783
- Swingedouw, D. and Braconnot, P.: Effect of the Greenland Ice-Sheet melting on the response and stability of the AMOC in the next century, *Geophysical Monograph Series*, 173, 20584–20589, 2007. 2765
- Swingedouw, D., Mignot, J., Braconnot, P., Mosquet, E., Kageyama, M., and Alkama, R.: Impact of Freshwater Release in the North Atlantic under Different Climate Conditions in an OAGCM, *J. Climate*, 22, 6377–6403, 2009. 2783
- Tarasov, L. and Peltier, W. R.: Greenland glacial history, borehole constraints, and Eemian extent, *J. Geophys. Res.*, 108, 2143, doi:10.1029/2001JB001731, 2003. 2767, 2793
- Vezina, J., Jones, B., and Ford, D.: Sea-level highstands over the last 500,000 years; evidence from the Ironshore Formation on Grand Cayman, British West Indies, *J. Sediment. Res.*, 69, 317–327, 1999. 2767
- Vizcaíno, M., Mikolajewicz, U., Gröger, M., Maier-Reimer, E., Schurgers, G., and Winguth, A.: Long-term ice sheet-climate interactions under anthropogenic greenhouse forcing simulated with a complex Earth System Model, *Clim. Dynam.*, 31, 665–690, 2008. 2784
- Weaver, A. J., Bitz, C. M., Fanning, A. F., and Holland, M. M.: THERMOHALINE CIRCULATION: High-Latitude Phenomena and the Difference Between the Pacific and Atlantic, *Annu. Rev. Earth Planet. Sci.*, 27, 231–285, 1999. 2765
- Wiersma, A. P. and Renssen, H.: Model-data comparison for the 8.2 ka BP event: confirmation of a forcing mechanism by catastrophic drainage of Laurentide Lakes, *Quaternary Sci. Rev.*, 25, 63–88, 2006. 2767, 2769

LIG climate and Greenland Ice Sheet melting

P. Bakker et al.

Title Page

Abstract

Introduction

Conclusions

References

Tables

Figures

◀

▶

◀

▶

Back

Close

Full Screen / Esc

Printer-friendly Version

Interactive Discussion



LIG climate and Greenland Ice Sheet melting

P. Bakker et al.

Title Page

Abstract

Introduction

Conclusions

References

Tables

Figures

◀

▶

◀

▶

Back

Close

Full Screen / Esc

Printer-friendly Version

Interactive Discussion



Table 1. Overview of estimated GIS contribution (m) to LIG sea-level high stand. Both proxy-data and combined model-data studies are listed.

Author	Range
Cuffey and Marshall (2000)	4–5.5
Tarasov and Peltier (2003)	2.7–4.5
Lhomme et al. (2005)	3.5–4.5
Otto-Bliesner et al. (2006)	1.9–3
Carlson et al. (2008)	2–5.5
Colville et al. (2011)	1.6–2.2

LIG climate and Greenland Ice Sheet melting

P. Bakker et al.

Table 2. Forcing applied to LIG climate simulations. Values are reconstructed for 130 ka BP, in line with PMIP3 agreements.

Orbital Parameters	Eccentricity	0.038209
	Obliquity	24.242°
	Perihelion-180°	228.32°
Greenhouse gas concentrations	CO ₂	257 ppm
	CH ₄	512 ppb
	N ₂ O	239 ppb
FWF sensitivity experiments		0.0065 Sv to 0.299 Sv

Title Page

Abstract

Introduction

Conclusions

References

Tables

Figures

◀

▶

◀

▶

Back

Close

Full Screen / Esc

Printer-friendly Version

Interactive Discussion



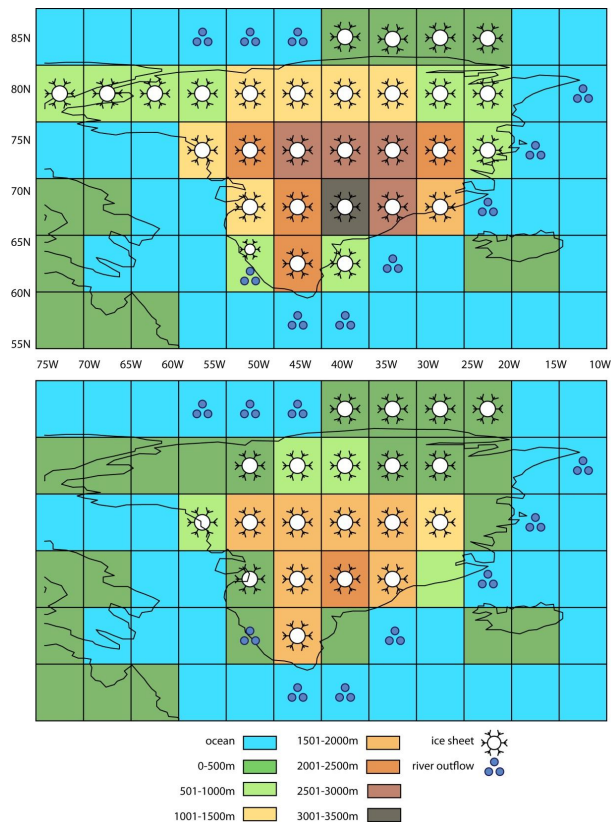


Fig. 1. Configuration of the GIS as used in the simulations. The PI (top panel) and LIG (lower panel) situations. The elevation of the different grid cells is given in green and brownish colours, the ocean grids cells are blue and different symbols indicate the river outflow points and the grid cells covered by ice. Many grid cells are partially covered with ocean and partially with land. For this figure, a cell is taken as ocean if at least 90 % of the cell is covered with ocean. The outlines of the continents are for reference only.

LIG climate and Greenland Ice Sheet melting

P. Bakker et al.

Title Page

Abstract

Introduction

Conclusions

References

Tables

Figures



Back

Close

Full Screen / Esc

Printer-friendly Version

Interactive Discussion



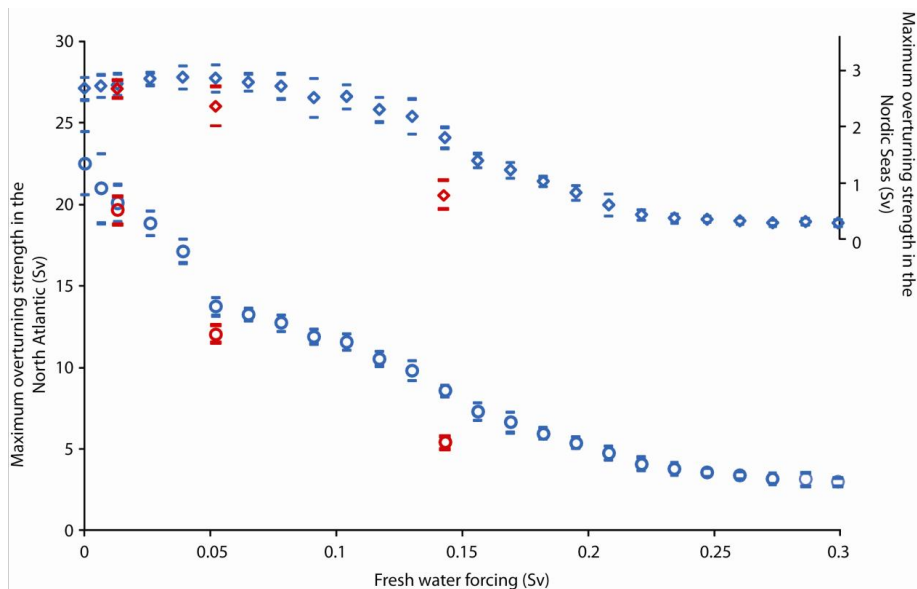


Fig. 2. The maximum strength of the overturning stream function (Sv) in the North Atlantic (circles) and Nordic Seas (diamonds) as a function of the freshwater forcing (Sv) from the GIS. The blue (red) symbols indicate simulations without (with) including changes in the topography and albedo of the GIS. Vertical bars indicate the 95 % confidence interval (2σ) calculated after a 10-yr running mean has been applied to filter out sub-decadal variability. All values are calculated over the last 150 yr of the simulations. Simulated Pre-industrial values are 23.65 ± 0.97 Sv and 2.76 ± 0.17 Sv for the maximum overturning strength in the North Atlantic and Nordic Seas respectively.

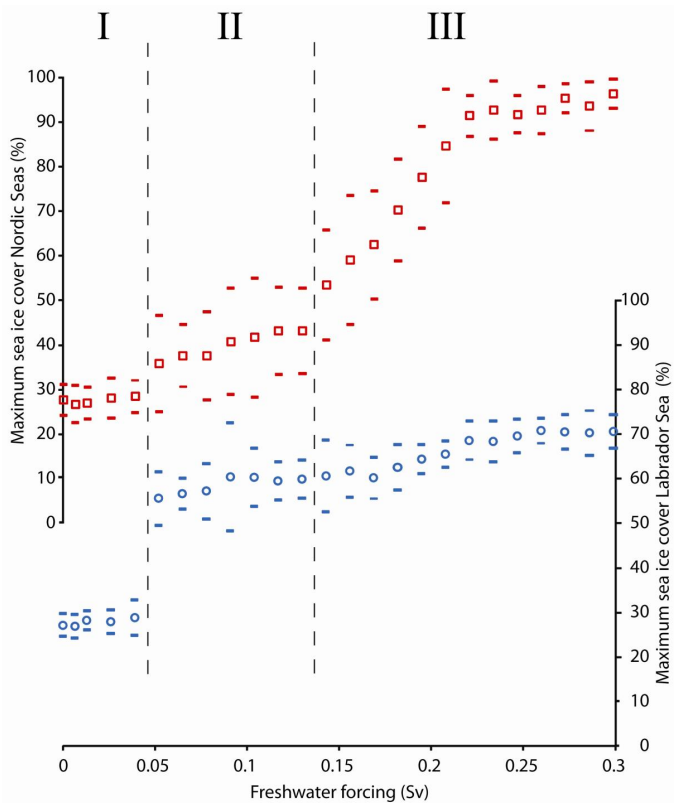


Fig. 3. Maximum (April) sea-ice cover (%) in the Labrador Sea (blue circles) and in the Nordic Seas (red squares) as a function of the melt rate of the GIS (Sv). Values are averages over the last 150 yr of the simulations. The vertical dashed lines distinguish the three different climate regimes.

LIG climate and Greenland Ice Sheet melting

P. Bakker et al.

Title Page

Abstract

Introduction

Conclusions

References

Tables

Figures

◀

▶

◀

▶

Back

Close

Full Screen / Esc

Printer-friendly Version

Interactive Discussion



LIG climate and Greenland Ice Sheet melting

P. Bakker et al.

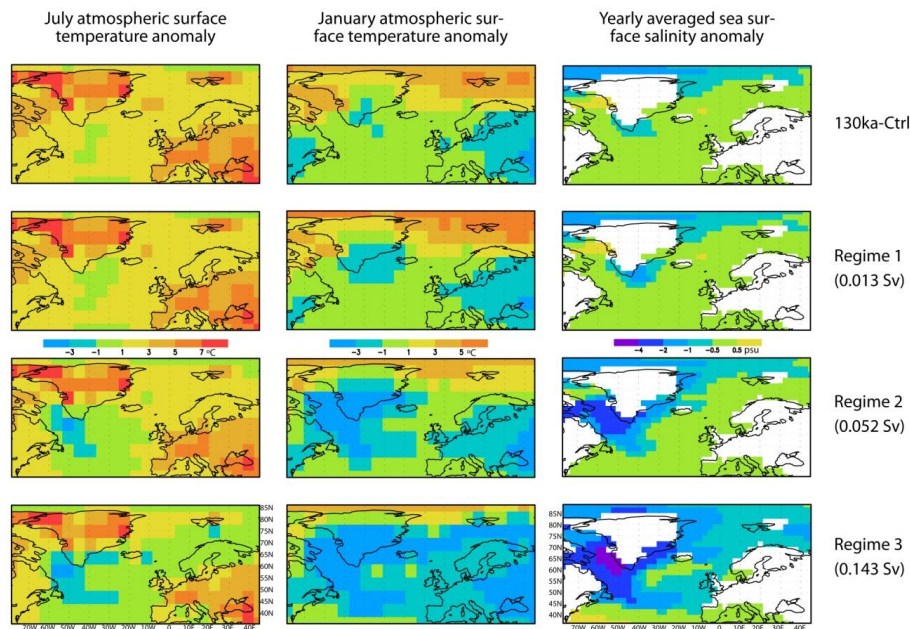


Fig. 4. Climate anomalies in the North Atlantic, in the North Atlantic region for the LIG-ctrl simulation (top panel) and the 3 climate and the 3 climate regimes, with respect to PI simulations. Left: July surface air temperatures ($^{\circ}\text{C}$); Middle: January surface air temperatures ($^{\circ}\text{C}$); Right: sea surface salinity (psu).

Title Page

Abstract

Introduction

Conclusions

References

Tables

Figures

◀

▶

◀

▶

Back

Close

Full Screen / Esc

Printer-friendly Version

Interactive Discussion



LIG climate and Greenland Ice Sheet melting

P. Bakker et al.

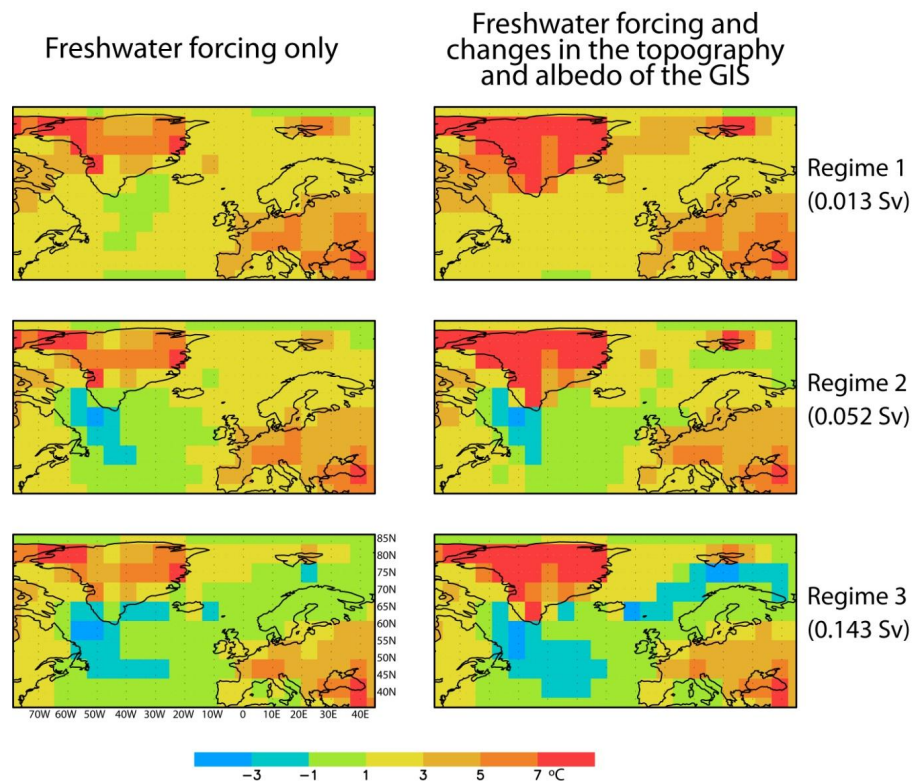


Fig. 5. Comparison of July surface air temperature anomalies ($^{\circ}\text{C}$) in the North Atlantic region for the 3 climate regimes (top to bottom) for simulations with either only FWF (left) or with both FWF and changes in the elevation and extent of the GIS (right).

Title Page

Abstract

Introduction

Conclusions

References

Tables

Figures

◀

▶

◀

▶

Back

Close

Full Screen / Esc

Printer-friendly Version

Interactive Discussion



LIG climate and Greenland Ice Sheet melting

P. Bakker et al.

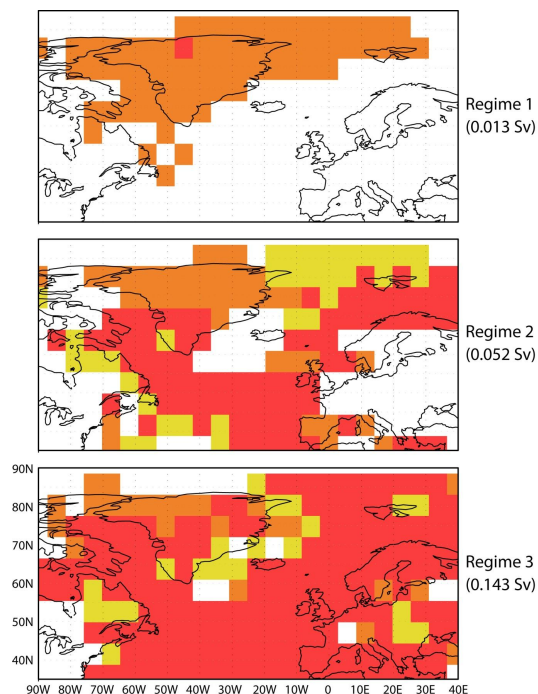


Fig. 6. For the 3 different climate regimes, the areas are shown where the FWF and/or changes in elevation and extent of the GIS significantly impact July surface air temperatures. Red indicates a significant FWF impact both with and without the additional influence of changes in elevation and extent of the GIS whereas orange (yellow) indicates that the impact is only significant in case the changes in elevation and extent of the GIS are (are not) included. Significant here means that with 96 % confidence (2σ) the forced July surface air temperature changes are larger than the unforced, internal variability of the LIG-ctrl simulation. On both the forced and unforced time-series a 10-yr running mean average has been applied to filter out all sub-decadal variability.

Title Page

Abstract

Introduction

Conclusions

References

Tables

Figures

◀

▶

◀

▶

Back

Close

Full Screen / Esc

Printer-friendly Version

Interactive Discussion



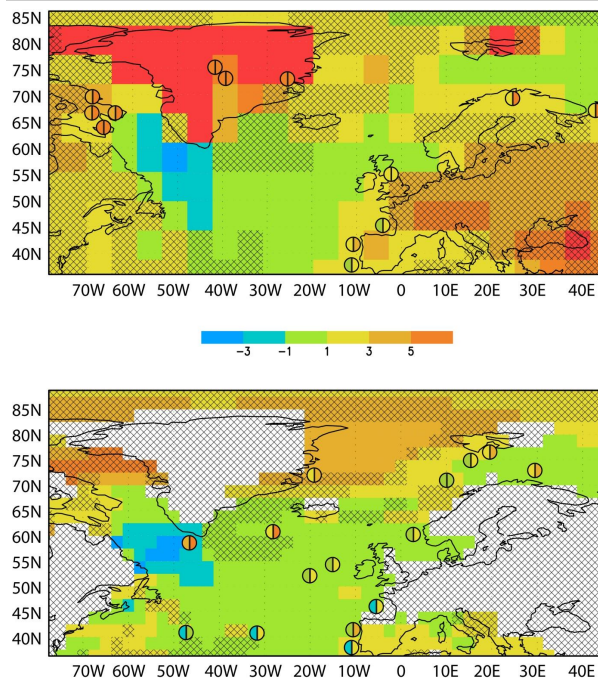


Fig. 7. Model-data comparison for July surface air temperature anomalies (upper panel) and August sea surface temperature anomalies (lower panel; °C) in regime 2 compared to PI including the impact of changes in elevation and extent of the GIS. In the shaded areas the simulated impact of the forcings is not significantly large (2σ ; 95 % confidence level) compared to the internal, decadal and multi-decadal variability. Proxies show maximum LIG summer temperatures from the CAPE-dataset (CAPE-members, 2006) complemented with data of Hillaire-Marcel et al. (2001) and Sánchez Goñi et al. (2008). Because of the coarse resolution of the model we have decided to incorporate several data points even though they fall at least partly outside of the significantly impacted area.